ACS Macro Letters

Letter

Cite This: ACS Macro Lett. 2019, 8, 1323−1327

pubs.acs.org/macroletters

Giant Hyaluronan Polymer Brushes Display Polyelectrolyte Brush Polymer Physics Behavior

Jessica L. Faubel,[†,‡] Riddhi P. Patel,[§] Wenbin Wei,[†,‡] Jennifer E. Curtis,[†,‡] and Blair K. Brettmann*[,§,∥]

[†]School of Physics, [‡]Parker H. Petit Institute for Bioengineering and Bioscience, [§]School of Materials Science and Engineering, and [∥]School of Chemical and Biomolecular Engineering, Georgia Institute of Technology, Atlanta, Georgia 30332, United States,

Supporting Information

ABSTRACT: Polyelectrolyte brushes are important stimuli-responsive materials in a variety of technological applications as well as in biological systems. Their small size, however, introduces characterization challenges, particularly in studying 3D structure and time-dependent behavior. In this Letter, we report on the polyelectrolyte brush behavior of extra-large hyaluronan brushes (∼15 μm) recently developed using an enzyme-mediated growth process. In response to increasing ionic strength, the brush displays the osmotic brush regime and the salted brush regime. We also show a collapse of 96% when the brush is placed in a poor solvent. This collapse is rapid when changing from a good to poor solvent, but re-expansion is slow when changing back to a good solvent. The observed brush behavior described in this Letter is similar to that seen for smaller polyelectrolyte brushes, indicating that these larger brushes may serve as model systems to study more complex phenomena through confocal microscopy.

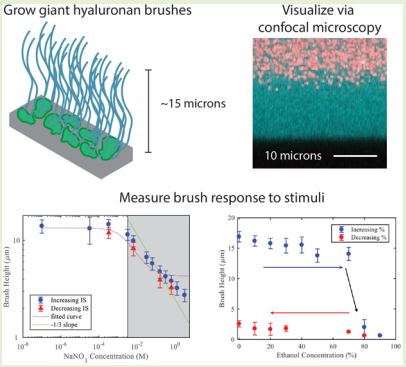

Polymer brushes provide enhanced functionality to surfaces for a variety of materials science applications. End-grafting of the polymer chains confines one end, but allows the other freedom of movement. Dense grafting causes deformation of the chains and extension away from the surface, forming a polymer brush. This enhances the scale of conformational changes by the polymer chains when solution conditions, such as solvent quality, are changed. When polyelectrolytes are used to form the brush, the stretching is even stronger and the brush size and configuration is sensitive to additional stimuli, such as ionic strength,[1] pH,[2] solvent,[3−6] and ion valency.[3−5] Polyelectrolyte brushes have been employed as antifouling surfaces,[6] used to control wettability and lubrication[7] and developed as biochemical sensors.[8,9] As the importance of brushes for these applications has increased, so has interest in the physical nature of the conformational changes and molecular level phenomena occurring as the local environment is changed.

Polyelectrolyte brushes are generally prepared through grafting to or grafting from approaches and are typically on the scale of tens to hundreds of nanometers, with rarer realizations into single-digit microns.[10−13] In examining stimuli-responsive behavior, the brush height is measured before and after changes in the environmental conditions. This is done through surface forces apparatus measurements,[1,14] ellipsometry,[15] quartz crystal microbalance with dissipation monitoring,[10,15] solution phase atomic force microscopy (AFM),[5,16] and fluorescent labeling of polymer chain ends.[17] Due to the small size of the brushes, experimental studies are typically limited to solely brush height measurements, though some measurements of polymer density as a function of distance from the grafting surface have been made through neutron reflectivity,[11] of 2D collapsed brush structure through AFM[5] and of the kinetics of brush collapse and expansion with ellipsometry.[15] It remains challenging to characterize detailed 3D brush conformations and time-dependent behavior of the brush when exposed to new stimuli.

Recently, giant, high density polyelectrolyte brushes of hyaluronan were synthesized using enzyme-mediated growth.[18] Hyaluronan (HA) is an anionic biopolymer composed of alternating *N*-acetyl-D-glucosamine and D-glucuronic acid that is present in a large number of human tissues and fluids and is a common material for tissue engineering[19,20] and therapeutics.[21] In nature, HA may be assembled in a brush configuration from a cell surface through the enzyme HA synthase,[22] where it is polymerized through addition of a monomer at the base of the polymer brush and extrusion of the HA polymer further through the cell membrane, a mechanism quite distinct from grafting to or grafting from (Figure 1).[23,24] By attaching HA synthase-rich membrane fragments on a glass support, HA brushes of up to 20 μm with a grafting density of approximately 0.0021 nm^{-2} were grown.[18] These giant polymer brushes are readily visualized through confocal microscopy, opening new avenues for studying 3D brush structure and time-dependent behavior.

A key characteristic of a polyelectrolyte brush is its response to solution ionic strength. At low ionic strengths, the brush is in the osmotic regime, where the large osmotic pressure difference between the counterions in the brush and the bulk

Received: July 10, 2019
Accepted: September 13, 2019
Published: September 25, 2019

Downloaded via GEORGIA INST OF TECHNOLOGY on July 23, 2020 at 15:08:52 (UTC).
See https://pubs.acs.org/sharingguidelines for options on how to legitimately share published articles.

© 2019 American Chemical Society

DOI: 10.1021/acsmacrolett.9b00530
ACS Macro Lett. 2019, 8, 1323−1327

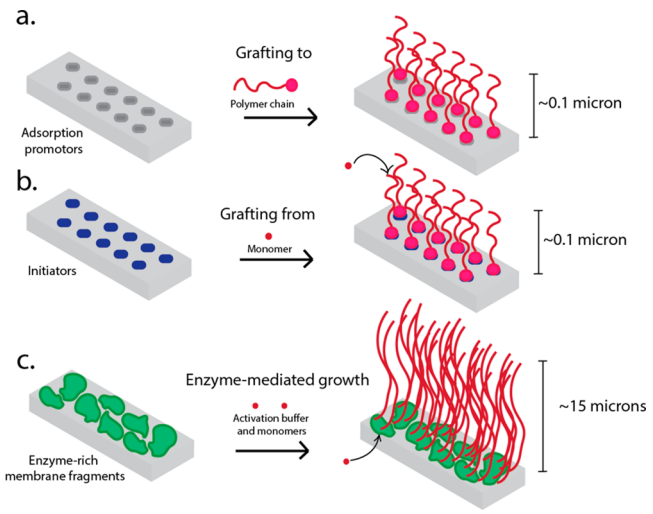

Figure 1. Illustration of three methods to form polymer brushes: (a) grafting to, where a preformed polymer chain adsorbs on the surface; (b) grafting from, where the chains are polymerized from initiators on the substrate and monomers are added to the growing chain end; and (c) enzyme-mediated growth, where chains are polymerized from enzyme-rich membrane fragments on the substrate and monomers are added at the base of the growing chain.

solution causes strong stretching of the chains and the brush height is constant with concentration. At higher salt concentrations, the brush enters the salted regime, where there is a power law dependence between brush height and ionic strength with an exponent of −1/3 due to the release of counterions that are localized in the brush in the osmotic regime, leading to the reduction in the osmotic pressure difference between the bulk and the brush. This exponent results from the balance of counterion osmotic pressure with Gaussian elasticity and neglects the excluded volume effect and finite chain extensibility. Finally, at very high salt concentrations, the brush behaves similarly to a neutral brush and the brush height is no longer a function of salt concentration.[1,24,25] To determine whether the HA brushes prepared through enzyme-mediated growth behave similarly to traditional polyelectrolyte brushes, we analyze their response to salt concentration in the context of the expected theoretical behavior.

The height of the brush as a function of $NaNO_3$ concentration was measured for HA brushes prepared through enzyme-mediated growth (Figure 2a). Brush height is measured directly with confocal visualization of excluded 200 nm nanoparticles as validated previously (Figure 2b).[18] Detailed methods describing brush preparation and the exclusion assay approach to brush height measurements are provided in the SI. Previous work showed that without further reinforcement, the brush can be damaged by rinsing. To stabilize the brush after growth, the sample is treated with EDC/NHS chemistry to generate covalent binding between carboxyl side groups on the HA and secondary amine groups on the underlying substrate. This binding results in reinforced brushes that are stable long-term and resistant to shear-induced brush height losses due to solvent exchanges.[18] Salt concentration studies for the nonreinforced brushes can be found in the Supporting Information, Figure S2. All experiments with the reinforced brush were performed on the same brush and the brush height as a function of $NaNO_3$ concentration is shown in Figure 2a.

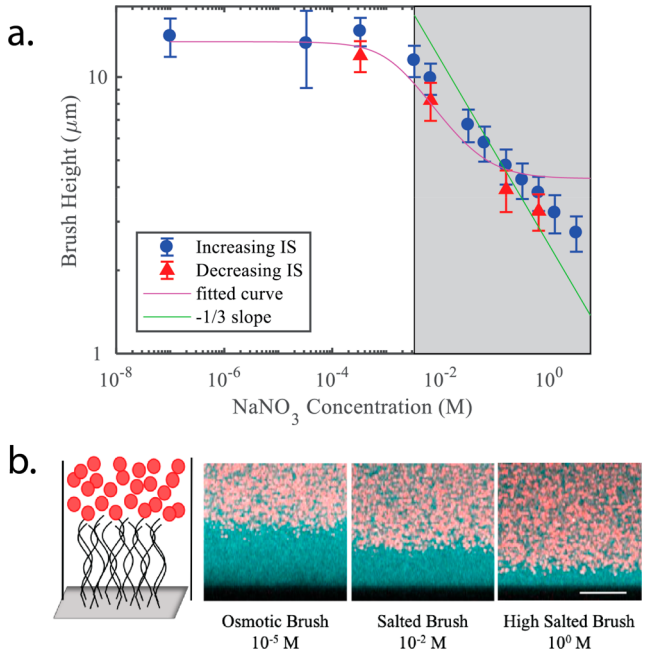

Figure 2. (a) Brush height as a function of $NaNO_3$ concentration for a reinforced HA brush prepared through enzyme-mediated growth (4 h growth time). Each data point represents at least four locations sampled on the brush. The lowest data point in the increasing ionic strength data is ultrapure water, assumed to have an ionic strength equivalent to 10^{-7} M $NaNO_3$ from H^+ ions. (b) *XZ* confocal microscope images of the brush cross section at 10^{-5}, 10^{-2}, and 10^0 M . Cyan coloring is fluorescent dextran ($R_g \sim 4$ nm) that penetrates the brush, effectively highlighting the brush, and red coloring is the excluded large beads. The substrate is black. Scale bar is 10 μm.

The reinforced brush exhibits the first two stages of polyelectrolyte brush behavior as the salt concentration is increased. At low salt concentrations, the brush height is constant at approximately 14 μm. At a $NaNO_3$ concentration of 0.003 M, the brush enters the salted brush regime and the height decreases with concentration with an apparent power law exponent of −0.210 ± 0.004. The neutral regime may have been reached at approximately 1 M, as the decrease in brush height as a function of concentration decreased, but we were unable to test at a sufficiently high salt concentration to verify due to the aggregation of the excluded beads at high salt concentrations. The brush regimes can also be clearly seen in the images in Figure 2b, where the cyan area is the brush, the red is the excluded beads and the black is the substrate. The brush is most extended in the osmotic regime, while it is least extended late in the salted brush regime.

The exponent for the power law dependence of height on salt concentration was shown experimentally to be −0.210 ± 0.004, lower than the theoretically predicted −1/3 slope. In the simple model that predicts the −1/3 exponent, the intrinsic excluded volume and finite chain extensibility were neglected.[25] Chen et al. developed a Flory-type mean-field model that takes into account these additional factors by defining the system as a balance of three pressures:

$$\pi_{cb} + \pi_{el} + \pi_{ev} = 0$$

where π_{cb} is the osmotic pressure of mobile ions, π_{el} is the elastic pressure, and π_{ev} is the pressure due to excluded volume.[26] Using the model described in Chen et al. with a fit parameter of $A = 5$, we calculated a theoretical curve for brush

DOI: 10.1021/acsmacrolett.9b00530
ACS Macro Lett. 2019, 8, 1323−1327

height vs salt concentration that accounts for excluded volume and chain extensibility (model details in Chen et al. and SI). A comparison of this curve to our experimental data in Figure 2a shows that this model is a better representation of the HA brush response to salt than the −1/3 power law exponent. This is also consistent with a study on a smaller "grafted to" HA brush (~2.5 μm), which showed that the experimental data fit well to a similar model where the excluded volume and finite extensibility were accounted for.[27] One distinction between the previous work on HA brushes and our work is that of polydispersity. The previous work focused on monodisperse brushes, whereas the brushes used in this work are distinctly polydisperse,[18] which could also contribute to the deviation of the model from the experimental data at the highest salt concentrations. Despite their extra-large size, the brushes prepared through enzyme-mediated growth behave similarly to smaller brushes prepared via a grafting to approach.

Solvent quality can also be used as a stimulus to influence brush behavior, with the brush being extended in a good solvent and collapsed in a poor solvent. Polyelectrolyte brushes display this behavior and are known to transition into a dense film at high grafting densities, to form pinned micelle (or octopus micelle) structures in a poor solvent at moderate grafting densities, and to assume single chain globule conformations at low grafting densities.[28] We used ethanol as a poor solvent for the HA backbone, which decreases the effective polyelectrolyte charge due to a decrease in the dielectric constant ($\varepsilon_{ethanol}$ = 24.5, ε_{water} = 80.1) and further decreases solubility through the dehydration of the side groups.[29,30] The maximum ethanol content achievable for testing is 90% due to water present in the fluorescent nanoparticle bead solution. Starting with a reinforced brush, we measured the height in pure water (16.2 ± 1.2 μm, st. dev.) and then removed the water, washed with ethanol three times and then monitored the brush height over 4 h. The brush height dropped abruptly to 0.70 ± 0.04 μm, a 96% decrease in thickness (Figure 3a). This is close to the resolution of the microscope (approximately 0.6 μm), so should be taken as an approximate value that represents a very collapsed brush.

A simple theoretical estimate for polyelectrolyte brush height in a poor solvent can be obtained if we assume a sufficiently dense brush that collapses homogeneously into a film.[27−29] Due to the very high degree of polymerization (~16200 for the brushes in this study) and the low grafting spacing (estimated to be approximately d = 22 nm within the fragment), we assume a dense brush, where the collapsed height may be estimated as $H = N\tau^{-1}d^{-2}a^3$ (N is the number of monomers, a is the monomer size (1 nm), and τ is the second virial coefficient indicating the solvent quality ($\tau = \chi^{-1/2}$)). This is the same approach as for a neutral brush, but has been shown to be a reasonable estimate for a fully collapsed, dense polyelectrolyte brush.[31] Using values of N = 16200 and d = 22 nm, as well as τ = 1/2 for a moderately poor solvent, we obtain an estimate for the brush height of a collapsed brush of 67 nm, or a 99.6% decrease in height from its contour length (16200 nm). This predicts greater brush shrinkage than that observed in the experiments (700 nm, 96%), which is expected for two reasons: (1) the limit of resolution of the confocal microscope method is ±600 nm, so we are at the limit in measuring the collapsed state and (2) the brush is in 90% ethanol/10% water, which still contains a significant amount of good solvent. It is known that the charges in polyelectrolyte brushes enable them to maintain their extended conformations

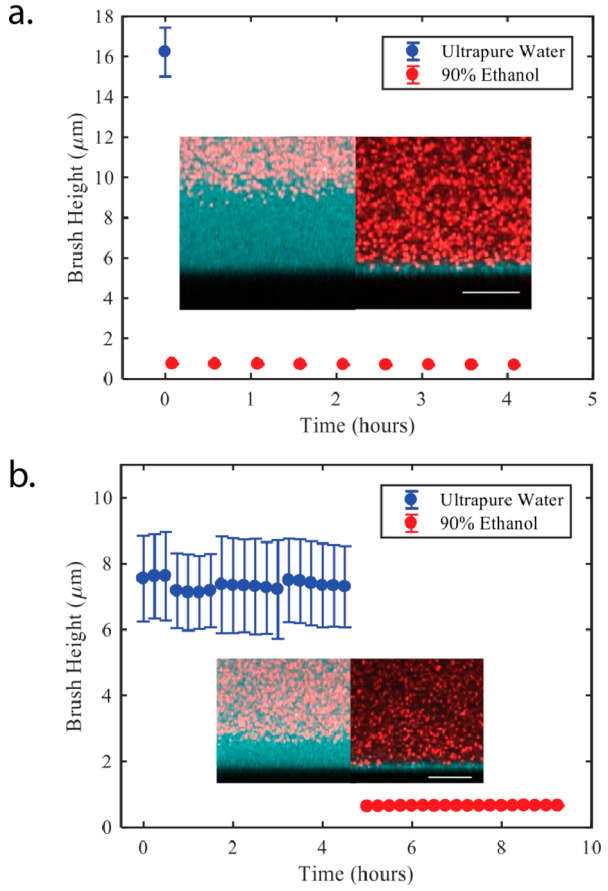

Figure 3. (a) Brush height over time through the first solvent exchange. Each data point represents five locations sampled on the brush. (b) Brush height over time through the second solvent exchange. Each data point represents 2−5 locations sampled on the brush. *XZ* confocal microscope images of the brush cross section in the different regimes are shown in the insets. Cyan coloring is fluorescent dextran that penetrates the brush, effectively highlighting the brush, and red coloring is the excluded large beads. The substrate is black. All scale bars are 10 μm.

in much poorer solvent environments than neutral polymers,[31] which can limit full collapse.

Further testing was done on the same brush sample to examine whether it could be re-expanded and recollapsed. To allow sufficient time for the brush to recover, it was stored in ultrapure water for 2 weeks, then rinsed three times with fresh ultrapure water and imaged. Figure 3b shows that the brush height returned partway to the height of the original measurements in water, with an average height of 8.1 ± 1.2 μm. The solvent was then switched to ethanol using three washes, and the brush height dropped immediately to 0.65 ± 0.03 μm, a 92% decrease in the brush height, consistent with the drop to 0.70 ± 0.04 μm (96% decrease) seen in the first solvent change to ethanol. This shows that re-expansion and collapse occur for the brush, but that the extent of re-expansion is limited, potentially due to slow diffusion of the good solvent into the thick, dense collapsed brush.

To examine the brush expansion and collapse further, we performed a gradual solvent exchange, moving from 100% water to 90% ethanol incrementally. The brush height remained similar to that of pure water up to the 80% ethanol-in-water solution, where it decreased to 2.02 μm compared to the height of the brush in pure water 16.9 μm

DOI: 10.1021/acsmacrolett.9b00530
ACS Macro Lett. 2019, 8, 1323−1327

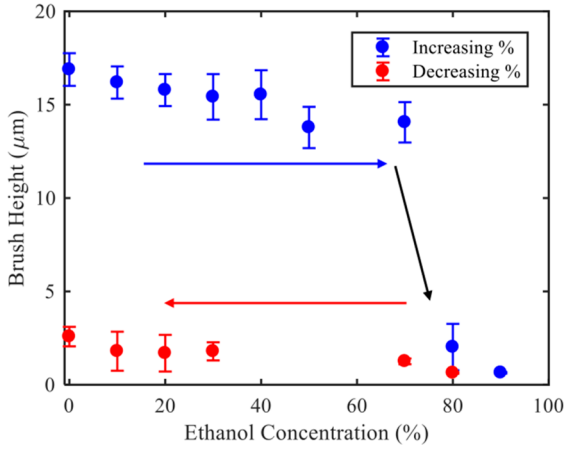

Figure 4. Brush height as a function of ethanol content. Blue data points indicate solvent exchanges proceeding from 0% to 90% (left to right) and red data points indicate solvent exchanges proceeding from 90% to 0% (right to left). Each data point represents at least four locations sampled on the brush.

(88% decrease; Figure 4). At 90% ethanol-in-water, the brush height decreased to 0.64 compared to the height of the brush in pure water 16.9 μm (96% decrease), identical to the 96% (16.2 to 0.70 μm) drop seen previously from water to 90% ethanol. This indicates that a critical amount of poor solvent is necessary to induce collapse. Interestingly, when the ethanol content is then dropped incrementally from 90% to 0%, the brush height does not recover. Unlike the prior experiment, here the brush was rinsed three times with each new solvent and imaged immediately, it was not allowed to incubate for hours in the new solvent. These results show a clear hysteresis in the brush collapse and expansion: when the brush collapses, it does so on the order of minutes, while when the brush re-expands, it only does so after long incubation periods, and even then, not fully.

In this Letter, we demonstrate that, despite the significantly larger size of the HA brushes prepared through enzyme-mediated growth, they behave similarly to other polyelectrolyte brushes, and we can observe this behavior using confocal microscopy. By examining the height of the brush as a function of salt concentration, we demonstrate that the brush displays the osmotic and salted brush regimes that are well-known for polyelectrolytes. We also examine the brush conformation in a poor solvent, showing that the brush undergoes a substantial decrease in height (>95%) in 90% ethanol/10% water compared to pure water. This collapse is rapid when changing from a good to a poor solvent, but re-expansion is very slow when changing back to the good solvent.

■ ASSOCIATED CONTENT

Supporting Information

The Supporting Information is available free of charge on the ACS Publications website at DOI: 10.1021/acsmacrolett.9b00530.

Experimental details, unreinforced brush results, and description of theoretical model (PDF)

■ AUTHOR INFORMATION

Corresponding Author

*E-mail: blair.brettmann@chbe.gatech.edu.

ORCID

Blair K. Brettmann: 0000-0003-1335-2120

Author Contributions

The manuscript was written through contributions of all authors. All authors have given approval to the final version of the manuscript.

Funding

Funding from NSF DMR 1709897, NSF PHYS 0955811 and NSF DMR 1205878.

Notes

The authors declare no competing financial interest.

■ ACKNOWLEDGMENTS

J.E.C. and J.L.F. gratefully acknowledge the National Science Foundation for financial support (Grant 1709897). J.E.C. and W.W. gratefully acknowledge the National Science Foundation for financial support (Grants 0955811 and 1205878). R.P.P. was supported by the Georgia Tech President's Undergraduate Research Award.

■ REFERENCES

(1) Balastre, M.; Li, F.; Schorr, P.; Yang, J.; Mays, J. W.; Tirrell, M. V. A Study of Polyelectrolyte Brushes Formed From Adsorption of Amphiphilic Diblock Copolymers Using the Surface Forces Apparatus. *Macromolecules* **2002**, *35* (25), 9480−9486.

(2) Sanjuan, S.; Perrin, P.; Pantoustier, N.; Tran, Y. Synthesis and Swelling Behavior of pH-Responsive Polybase Brushes. *Langmuir* **2007**, *23* (10), 5769−5778.

(3) Brettmann, B. K.; Laugel, N.; Hoffmann, N.; Pincus, P.; Tirrell, M. Bridging Contributions to Polyelectrolyte Brush Collapse in Multivalent Salt Solutions. *J. Polym. Sci., Part A: Polym. Chem.* **2016**, *54* (2), 284−291.

(4) Brettmann, B.; Pincus, P.; Tirrell, M. Lateral Structure Formation in Polyelectrolyte Brushes Induced by Multivalent Ions. *Macromolecules* **2017**, *50* (3), 1225−1235.

(5) Yu, J.; Jackson, N. E.; Xu, X.; Brettmann, B. K.; Ruths, M.; de Pablo, J. J.; Tirrell, M. Multivalent Ions Induce Lateral Structural Inhomogeneities in Polyelectrolyte Brushes. *Science Advances* **2017**, *3* (12), 1−11.

(6) Yadav, V.; Jaimes-Lizcano, Y. A.; Dewangan, N. K.; Park, N.; Li, T.-H.; Robertson, M. L.; Conrad, J. C. Tuning Bacterial Attachment and Detachment via the Thickness and Dispersity of a pH-Responsive Polymer Brush. *ACS Appl. Mater. Interfaces* **2017**, *9* (51), 44900−44910.

(7) Raviv, U.; Giasson, S.; Kampf, N.; Gohy, J.-F.; Jerome, R.; Klein, J. Lubrication by Charged Polymers. *Nature* **2003**, *425* (6954), 163−165.

(8) Fan, R.; Vermesh, O.; Srivastava, A.; Yen, B. K H; Qin, L.; Ahmad, H.; Kwong, G. A; Liu, C.-C.; Gould, J.; Hood, L.; Heath, J. R Integrated Barcode Chips for Rapid, Multiplexed Analysis of Proteins in Microliter Quantities of Blood. *Nat. Biotechnol.* **2008**, *26* (12), 1373−1378.

(9) Drummond, T. G.; Hill, M. G.; Barton, J. K. Electrochemical DNA Sensors. *Nat. Biotechnol.* **2003**, *21* (10), 1192−1199.

(10) Azzaroni, O.; Moya, S.; Farhan, T.; Brown, A. A.; Huck, W. T. S. Switching the Properties of Polyelectrolyte Brushes via "Hydrophobic Collapse. *Macromolecules* **2005**, *38*, 10192−10199.

(11) Yu, J.; Mao, J.; Yuan, G.; Satija, S.; Jiang, Z.; Chen, W.; Tirrell, M. Structure of Polyelectrolyte Brushes in the Presence of Multivalent Counterions. *Macromolecules* **2016**, *49* (15), 5609−5617.

(12) Yu, J.; Mao, J.; Yuan, G.; Satija, S.; Chen, W.; Tirrell, M. The Effect of Multivalent Counterions to the Structure of Highly Dense Polystyrene Sulfonate Brushes. *Polymer* **2016**, *98* (C), 448−453.

(13) Gelbert, M.; Biesalski, M.; Rühe, J.; Johannsmann, D. Collapse of Polyelectrolyte Brushes Probed by Noise Analysis of a Scanning Force Microscope Cantilever. *Langmuir* **2000**, *16* (13), 5774−5784.

DOI: 10.1021/acsmacrolett.9b00530
ACS Macro Lett. 2019, 8, 1323−1327

(14) Farina, R.; Laugel, N.; Pincus, P.; Tirrell, M. Brushes of Strong Polyelectrolytes in Mixed Mono- and Tri-Valent Ionic Media at Fixed Total Ionic Strengths. *Soft Matter* **2013**, *9* (44), 10458−10472.
(15) Cheesman, B. T.; Smith, E. G.; Murdoch, T. J.; Guibert, C.; Webber, G. B.; Edmondson, S.; Wanless, E. J. Polyelectrolyte Brush pH-Response at the Silica-Aqueous Solution Interface: a Kinetic and Equilibrium Investigation. *Phys. Chem. Chem. Phys.* **2013**, *15* (34), 14502−14509.
(16) Farhan, T.; Azzaroni, O.; Huck, W. AFM Study of Cationically Charged Polymer Brushes: Switching Between Soft and Hard Matter. *Soft Matter* **2005**, *1*, 66−68.
(17) Bracha, D.; Bar-Ziv, R. H. Dendritic and Nanowire Assemblies of Condensed DNA Polymer Brushes. *J. Am. Chem. Soc.* **2014**, *136* (13), 4945−4953.
(18) Wei, W.; Faubel, J. L.; Selvakumar, H.; Kovari, D. T.; Tsao, J.; Rivas, F.; Mohabir, A. T.; Krecker, M.; Rahbar, E.; Hall, A. R.; Filler, M. A.; Washburn, J. L.; Weigel, P. H.; Curtis, J. E. Self-Regenerating Giant Hyaluronan Polymer Brushes. *Submitted*. 2019.
(19) Allison, D. D.; Grande-Allen, K. J. Review. Hyaluronan: a Powerful Tissue Engineering Tool. *Tissue Eng.* **2006**, *12* (8), 2131−2140.
(20) Collins, M. N.; Birkinshaw, C. Hyaluronic Acid Based Scaffolds for Tissue Engineering—a Review. *Carbohydr. Polym.* **2013**, *92* (2), 1262−1279.
(21) Karbownik, M. S.; Nowak, J. Z. Hyaluronan: Towards Novel Anti-Cancer Therapeutics. *Pharmacol. Rep.* **2013**, *65* (5), 1056−1074.
(22) Boehm, H.; Mundinger, T. A.; Boehm, C. H.; Hagel, V.; Rauch, U.; Spatz, J. P.; Curtis, J. E. Mapping the mechanics and macromolecular organization of hyaluronan-rich cell coats. *Soft Matter* **2009**, *5* (21), 4331−4337.
(23) Bohaumilitzky, L.; Huber, A.-K.; Stork, E. M.; Wengert, S.; Woelfl, F.; Boehm, H. A Trickster in Disguise: Hyaluronan's Ambivalent Roles in the Matrix. *Front. Oncol.* **2017**, *7*, 629−19.
(24) Weigel, P. H. Hyaluronan Synthase: the Mechanism of Initiation at the Reducing End and a Pendulum Model for Polysaccharide Translocation to the Cell Exterior. *Int. J. Cell Biol.* **2015**, *2015* (26), 1−15.
(25) Borisov, O. V.; Zhulina, E. B.; Birshtein, T. M. Diagram of the States of a Grafted Polyelectrolyte Layer. *Macromolecules* **1994**, *27*, 4795−4803.
(26) Chen, L.; Merlitz, H.; He, S.-Z.; Wu, C.-X.; Sommer, J.-U. Polyelectrolyte Brushes: Debye Approximation and Mean-Field Theory. *Macromolecules* **2011**, *44* (8), 3109−3116.
(27) Attili, S.; Borisov, O. V.; Richter, R. P. Films of End-Grafted Hyaluronan Are a Prototype of a Brush of a Strongly Charged, Semiflexible Polyelectrolyte with Intrinsic Excluded Volume. *Biomacromolecules* **2012**, *13* (5), 1466−1477.
(28) Williams, D. R. M. Grafted Polymers in Bad Solvents: Octopus Surface Micelles. *J. Phys. II* **1993**, *3* (9), 1313−1318.
(29) Lago, G.; Oruna, L.; Cremata, J.; Perez, C.; Coto, G.; Lauzan, E.; Kennedy, J. Isolation, Purification and Characterization of Hyaluronan From Human Umbilical Cord Residues. *Carbohydr. Polym.* **2005**, *62* (4), 321−326.
(30) Yang, P.-F.; Lee, C.-K. Hyaluronic Acid Interaction with Chitosan-Conjugated Magnetite Particles and Its Purification. *Biochem. Eng. J.* **2007**, *33* (3), 284−289.
(31) Ross, R. S.; Pincus, P. The Polyelectrolyte Brush: Poor Solvent. *Macromolecules* **1992**, *25* (8), 2177−2183.

DOI: 10.1021/acsmacrolett.9b00530
ACS Macro Lett. 2019, 8, 1323−1327